

# HUMIDITY AND TEMPERATURE PROFILES FROM MIXED RETRIEVAL METHOD, ECMWF ANALYSIS, AND RADIOSONDES

B. B. Stankov,  
NOAA/Environmental Technology Laboratory,  
Boulder, Co., USA

## 1. INTRODUCTION

Mixing retrieval method (MRM), is advanced to obtain humidity and temperature profiles with improved accuracy and reliability from diverse ground-based remote sensing measurements and the *TIROS-N* (Television and Infrared Observational Satellite) Operational Vertical Sounder (TOVS) measurements. While humidity and temperature have been identified as major variables in assessing climatic change and they play a fundamental role in Earth's energy and water cycle processes (Starr and Melfi, 1991; Dabberdt and Schlatter 1996) current observing systems (operational radiosonde network and satellites) are inadequate. The current radiosonde observing system does provide high quality measurements of the atmospheric state, but coverage is very limited. On the other hand, polar orbiting satellite-based systems provide global coverage, but have poor vertical and temporal resolution within the planetary boundary layer (PBL), especially in its upper part where there is large humidity flux between the PBL and the free atmosphere.

The new MRM combines upper atmosphere information of the satellite-based systems with the high resolution of the ground-based systems for the lower atmosphere and the in situ observations from commercial airliners covering the middle atmosphere. As the number of the ground-based remote sensing radars around the globe increases, MRM can also truly take advantage of the satellite's global coverage.

In this paper we compare the humidity and temperature profiles for 20 cases using the MRM profiles, and the profiles obtained from the European Centre for Medium-range Weather Forecast (ECMWF) analysis, with the 20 profiles obtained from research radiosonde ascents.

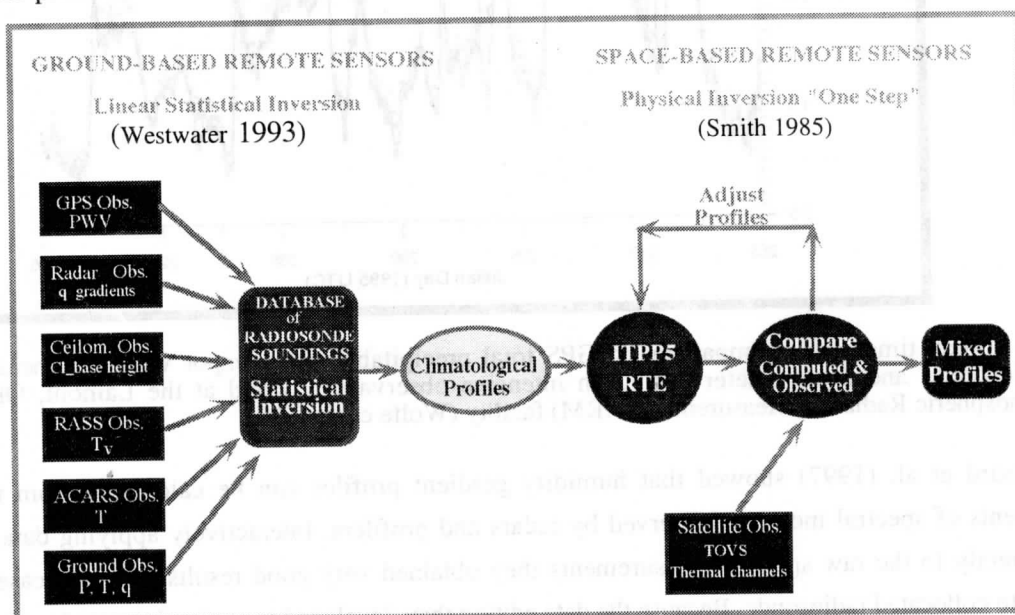


Figure 1. Mixing Retrieval Method (MRM).

## 2. METHOD

### 2.1 Mixing Retrieval Method

MRM (Fig. 1) combines linear statistical retrieval method (Westwater 1993) applied to the ground-based remote sensing measurements with the International TOVS Processing Package (ITPP) physical retrieval method (Smith 1985) applied to the space-based measurements from the polar orbiting satellites. Profiles of humidity gradients observed by a 449 MHz wind profiler system are combined with Global Positioning System (GPS) measurements of total precipitable water vapor, Radio Acoustic Sounding System (RASS) measurements of virtual temperature, and standard surface meteorological measurements to retrieve temperature and humidity profiles from ground-based measurements. These climatological profiles (Fig. 1) are then used as the first-guess profiles within the ITTP to obtain MRM humidity and temperature profiles.

In a previous study (Stankov 1996), employing ground- and space-based measurements were used to retrieve temperature and humidity profiles, ground-based microwave radiometer measurements were used instead of GPS measurements to calculate path-integrated water vapor. Radar-observed humidity gradient profile measurements were not available at the time. This study found that the retrieved temperature profiles showed excellent agreement with radiosonde-observed temperature profiles. However, retrieved humidity profiles showed no ability to detect sharp changes associated with shallow dry or moist atmospheric layers.

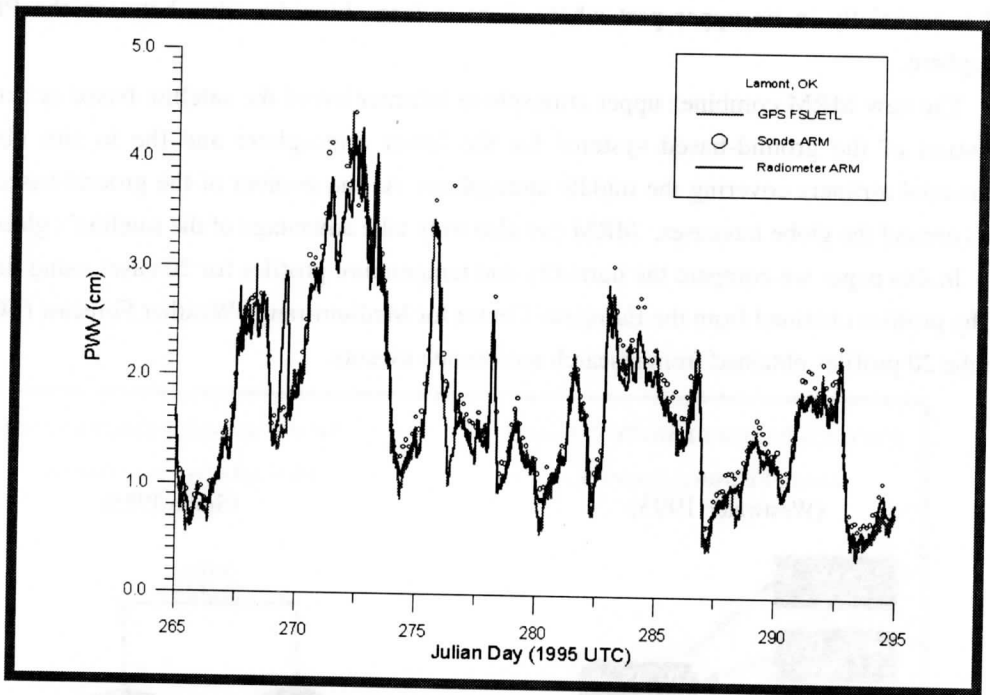


Fig. 2. A 30-day time-series comparison of GPS total precipitable water vapor with that measured by radiosondes and a radiometer during an intensive observation period at the Lamont, Oklahoma Atmospheric Radiation Measurement (ARM) facility (Wolfe et al. 1997).

Gossard et al. (1997) showed that humidity gradient profiles can be calculated from the raw measurements of spectral moments observed by radars and profilers. Interactively applying data quality control directly to the raw spectral measurements they obtained very good results for three cases when compared to collocated radiosonde. Because the data editing they developed is not implemented routinely

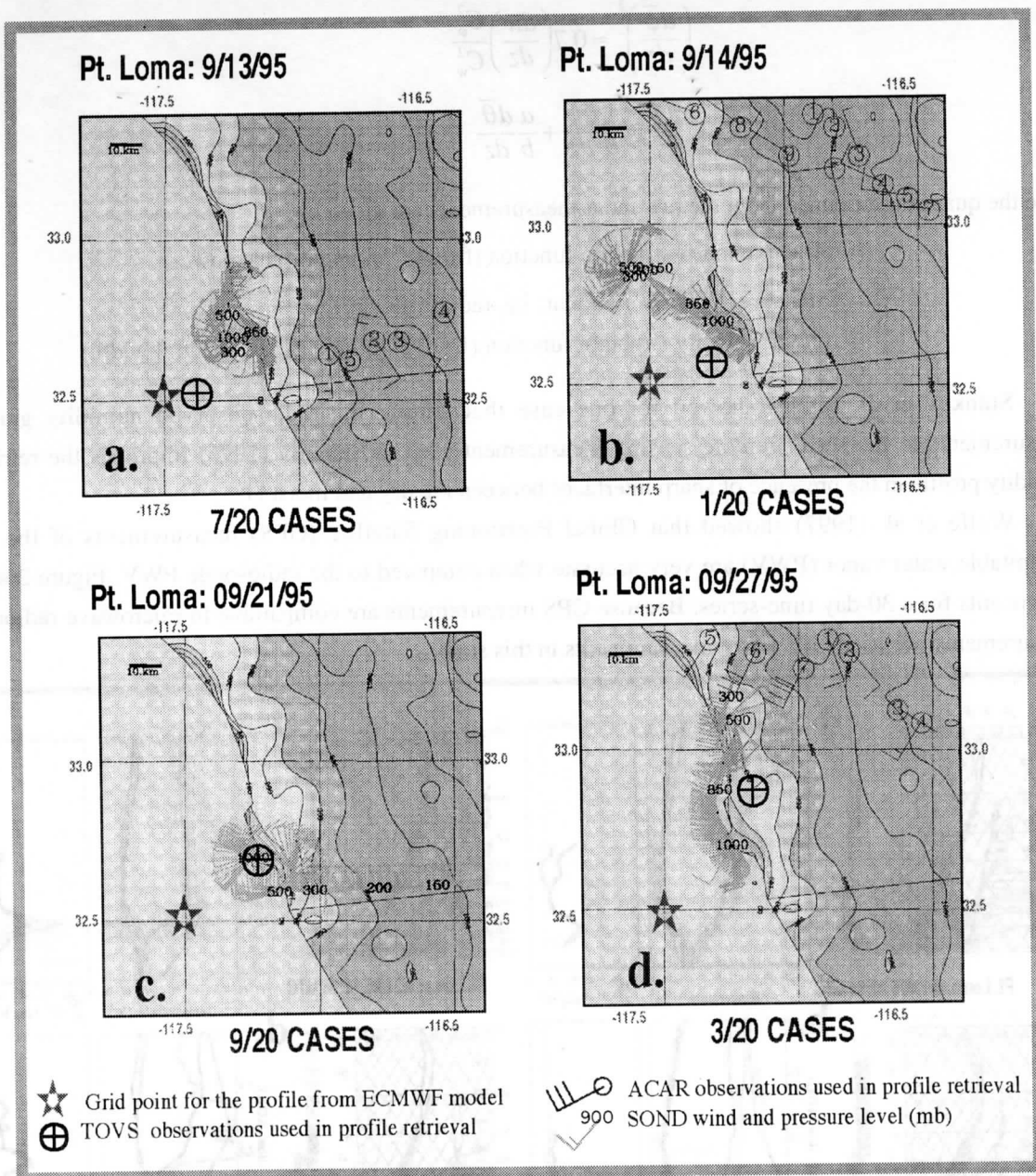


Fig. 3. Four out of twenty typical cases obtained during the 1995 Point Loma Experiment. a.) Radiosondes remained in the area of the ground-based measurements after reaching levels above PBL, b.) Radiosondes moved over the ocean above PBL c.) Radiosondes carried away eastward by the jet stream after reaching levels above PBL, d.) radiosondes moved northward along the shore after reaching levels above PBL.

yet, raw radar-observed moment measurements are used in the present study. Radar moment measurements are contaminated by insects, birds, airplanes, etc. However, applying the robust exploratory data analyses techniques based on the statistics of the median rather than the mean (Velleman and Hoaglin 1981), to profiler moment data yielded humidity gradient profile measurements for the entire set of 20 cases. Eq. 1 gives the expression for the gradient of the potential refractive index,  $\phi$ . If in addition, the gradient of the potential temperature ( $\theta$ ) is known from RASS measurements the gradient of humidity ( $Q$ ) can be obtained from the Eq. 2.

$$\left(\frac{d\bar{\phi}}{dz}\right)^2 \approx 0.7 \left(\frac{d\bar{u}}{dz}\right) \frac{C_\phi^2}{C_w^2} \tag{1}$$

$$\frac{\partial \bar{Q}}{\partial z} = \frac{1}{b} \frac{d\bar{\phi}}{dz} + \frac{a}{b} \frac{d\bar{\theta}}{dz} \tag{2}$$

Here the quantities obtained from the raw radar measurements are given by:

- $C_\phi^2$  = refractive index structure function (from 0<sup>th</sup> moment, i.e., power)
- $\frac{d\bar{u}}{dz}$  = wind shear (from 1<sup>st</sup> moment, i.e. radial velocity)
- $C_w^2$  = vertical velocity structure function (from 2<sup>nd</sup> moment, i.e. spectral width)

Stankov et al. (1996) showed for one case that adding the radar-observed humidity gradient measurements to the set of remote sensing measurement used in Stankov (1996) improves the retrieved humidity profile in the presence of sharp interfaces between the dry and moist air.

Wolfe et al. (1997) showed that Global Positioning Satellite (GPS) measurements of the total precipitable water vapor (PWV) are very accurate when compared to the radiosonde PWV. Figure 2 shows their results for a 30-day time-series. Because GPS measurements are comparable to microwave radiometer measurements, we used GPS PWV measurements in this study.

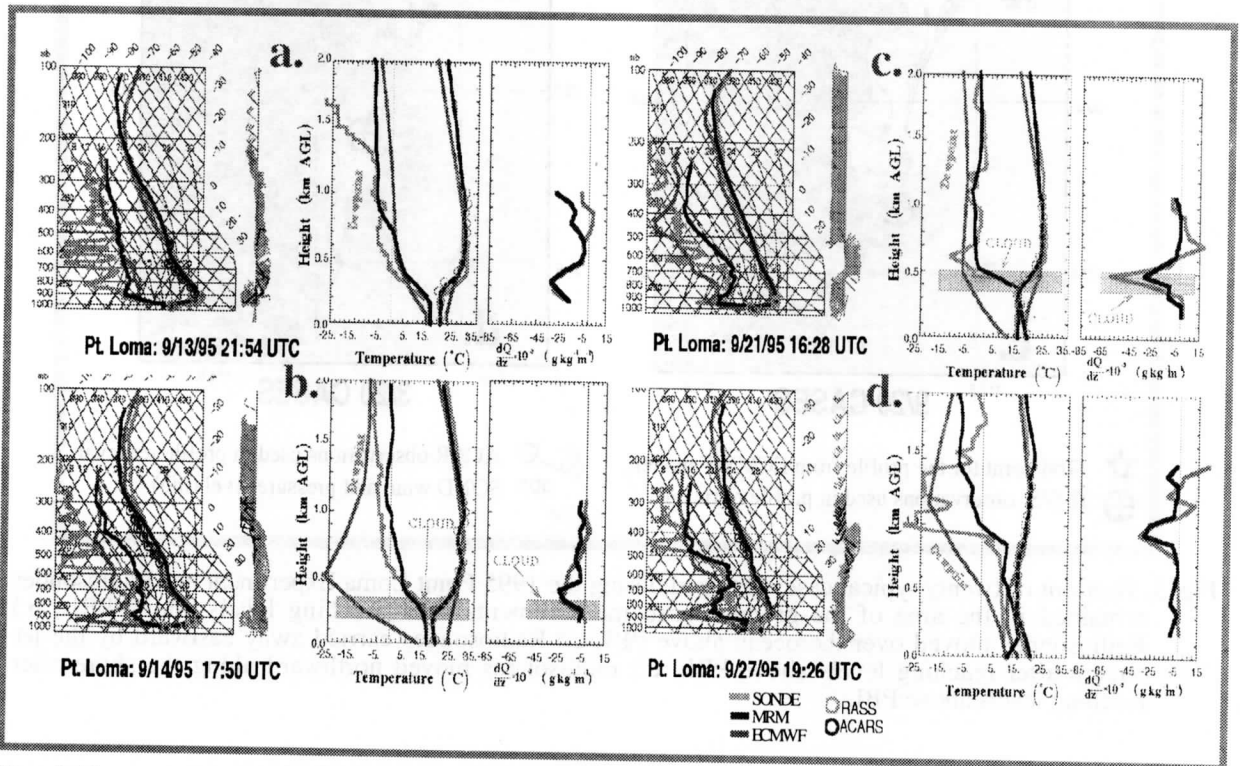


Fig. 4. Temperature, humidity, and  $dQ/dz$  profiles for the cases in Fig. 3. Each case consists of SkewT-logP diagram, linear plot of temperature and humidity, and a linear plot of  $dQ/dz$ .

## 2.2 One-dimensional Variational Analysis Method (1DVAR)

This method was developed and implemented in 1992 by the ECMWF (Eyre 1993, MacNally 1993) specifically to handle TOVS radiances. It seeks to find an atmospheric state that gives best fit to available satellite radiance observations and background Numerical Weather Prediction (NWP) information (to within their respective errors) while applying appropriate additional constraints concerned with dynamic or physical

processes. This is accomplished by minimizing a cost function that measures the departure of analyzed state from the observations, the background, and other information. The vertical resolution of the temperature and humidity fields obtained from 1DVAR are determined by the model's vertical resolution, which in the ECMWF's case means 31 levels between 1000 mb and 10 mb levels.

1DVAR makes it possible to assimilate observations of parameters not explicitly carried in the models (i.e. TOVS radiance measurements). This is significant to the ground-based remote sensing research community because it allows for the inclusion of any number of non-conventional measurements such as humidity gradient profiles, vertical cloud distribution, cloud particle size distribution, RASS temperature measurements or any new development in the future.

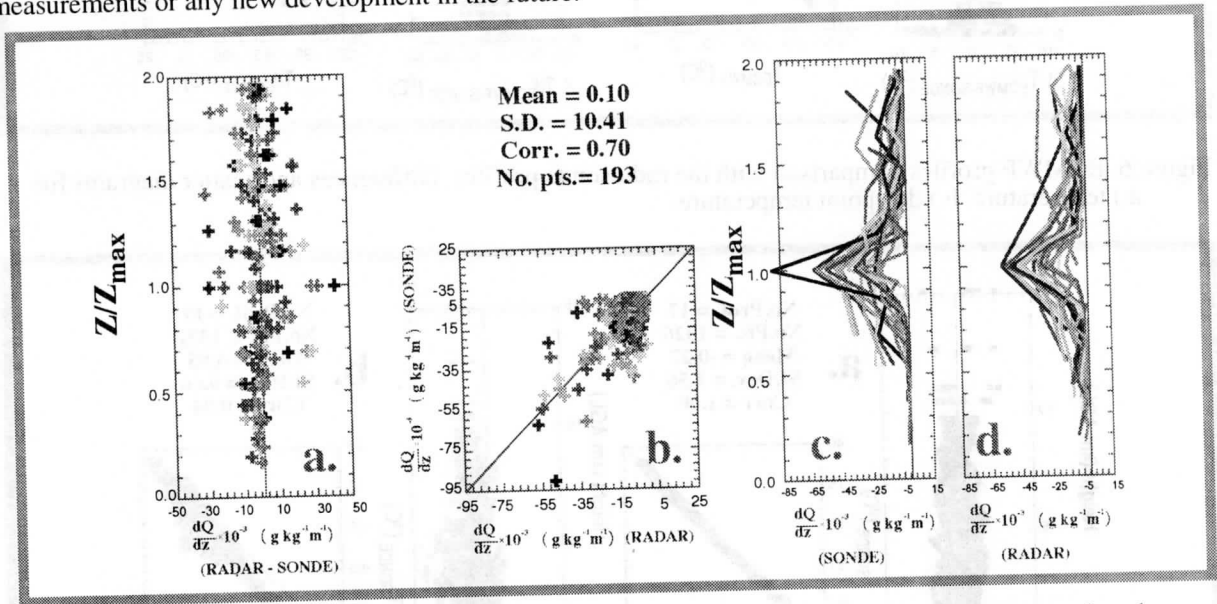


Figure 5.  $dQ/dz$  statistics for the entire dataset of 20 soundings. a.) Differences between radar-observed  $dQ/dz$  and computed from the radiosonde ascents. b.) Scatter diagram for the radar-observed  $dQ/dz$  and computed from the radiosonde ascents. c.)  $abs(dQ/dz)$  computed from the radiosonde ascents. d.)  $abs(dQ/dz)$  radar-observed  $dQ/dz$ . The vertical coordinate is scaled with the PBL height.

### 3. EXPERIMENT

An experiment was conducted in the stable maritime air of southern California from 24 August to 27 September 1995 to study the ability of the wind profiling radar combined with the RASS system to measure profiles of the humidity gradient from the radar-measured moment data. Climatological large-scale subsidence and dry air aloft at this time of year produce the PBL that is topped by a very sharp and strong vertical moisture and temperature gradients thus ideally suited for this study. Because we were able to obtain additional data it was possible to retrieve humidity and temperature profiles using the humidity gradient measurements as an additional constraint within the MRM. This allowed determination of the humidity gradient profile contribution to the accuracy of the humidity profile retrievals.

During the month-long period the System Demonstration and Integration Division (SDID) of the Environmental Technology Laboratory at the National Oceanic and Atmospheric Administration (NOAA) collected 20 cases for the analysis. Figure 3 shows the four categories of the radiosonde ascents, the ECMWF analysis grid point used for comparison, TOVS grid point used in MRM retrieval, and the location of ACARS measurements. The primary difference between these cases is the sonde trajectory, which relates to a given synoptic situation.

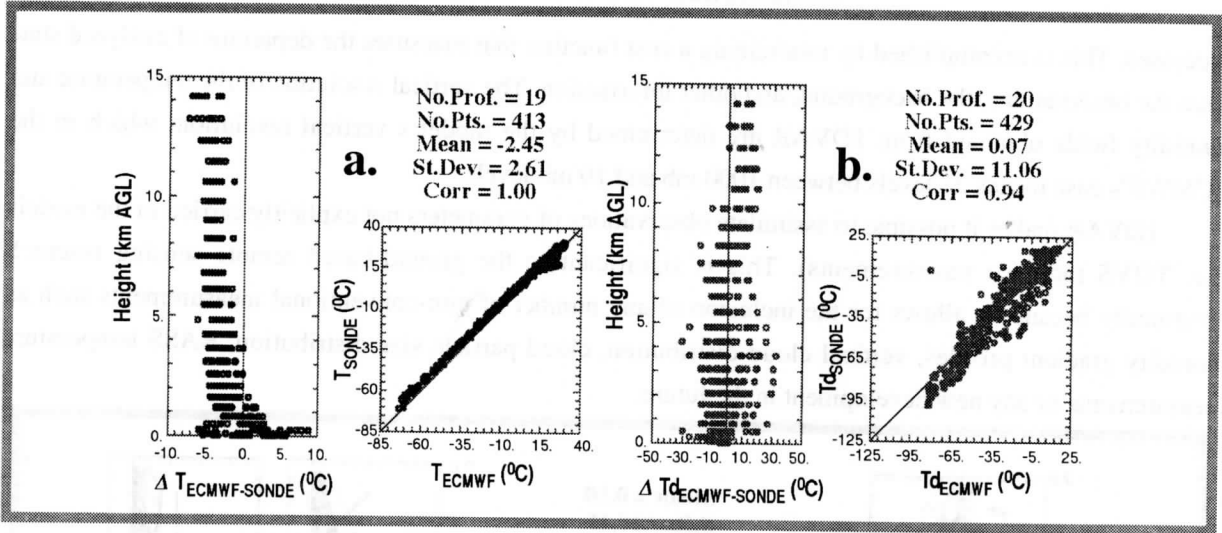


Figure 6. ECMWF profiles comparison with the radiosonde profiles. Differences and scatter diagrams for a.) temperature, b.) dewpoint temperature.

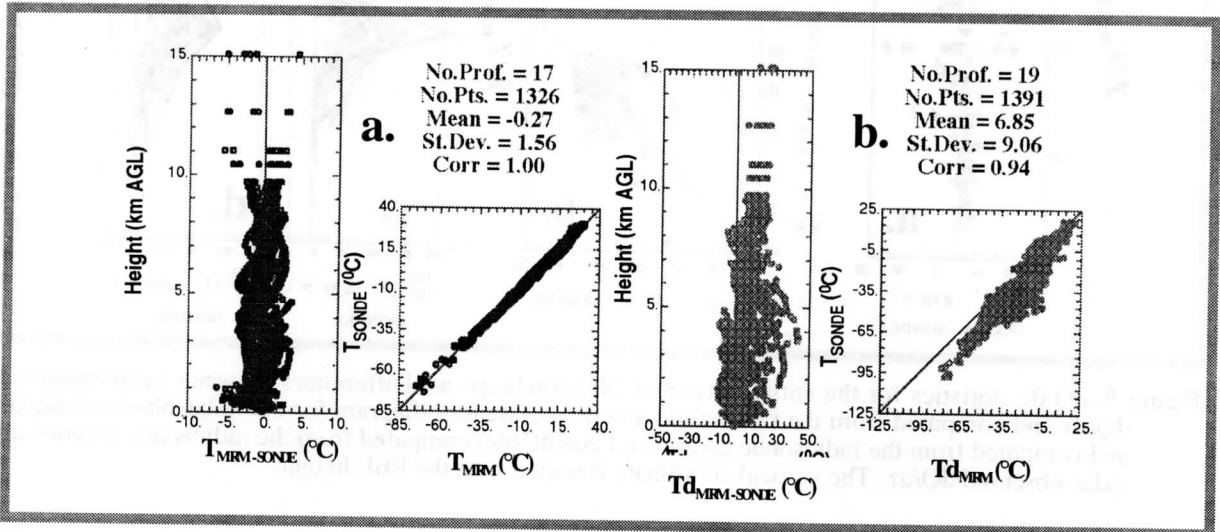


Figure 7. MRM profiles comparison with the radiosonde profiles. Differences and scatter diagrams for a.) temperature, b.) dewpoint temperature.

#### 4. RESULTS

##### 4.1 Individual Profiles

Figure 4 shows comparison of individual humidity, temperature, and humidity gradient profiles for each category in Fig. 3. Each case contains three plots. The left-hand side represents the SkewT-logP diagram showing the profiles up to 100 mb level. The middle plot shows a linear plot of the same retrieved, ECMWF, and radiosonde profiles up to 2 km AGL to emphasize the details at the top of PBL. The right hand plot shows the radar-observed humidity gradient compared with the humidity gradient computed from the radiosonde ascent. From all four cases it is evident that the inclusion of the humidity gradient profile in the MRM provides a humidity profile that accurately represents the state of the atmosphere within the PBL. The profiles obtained from the ECMWF mode+(1DVAR analysis method) do not show the same detailed vertical structure achieved by the MRM profiles.

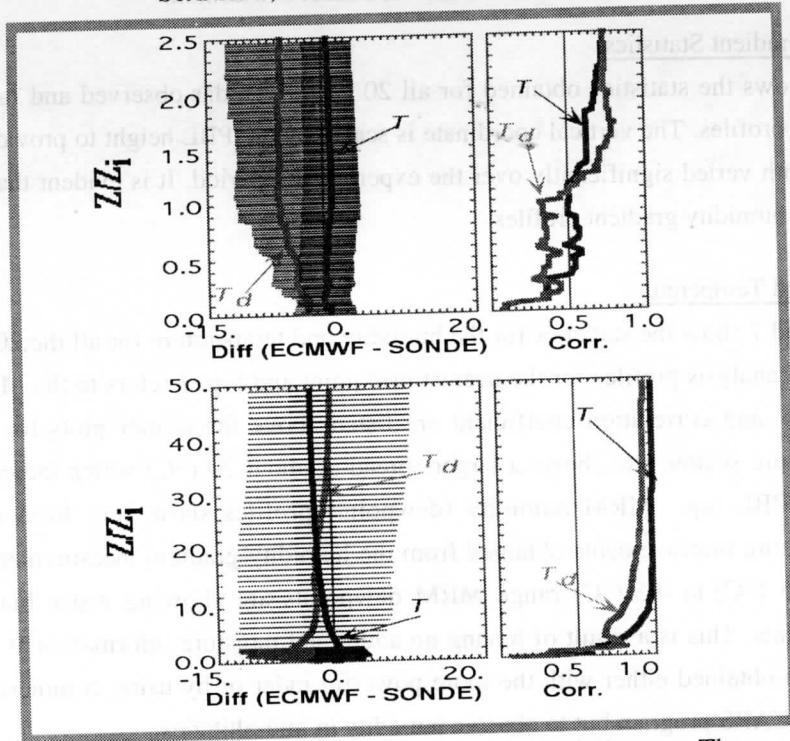


Figure 8 ECMWF profile comparison with radiosonde profiles for all 20 cases. The mean (thick solid line) and standard deviations (thin, horizontal solid lines) of the differences and the correlation coefficient (thick solid line) for all levels  $Z$  normalized to the PBL height  $Z_i$ . Top  $Z/Z_i = 2.5$ . Bottom  $Z/Z_i = 50$ .

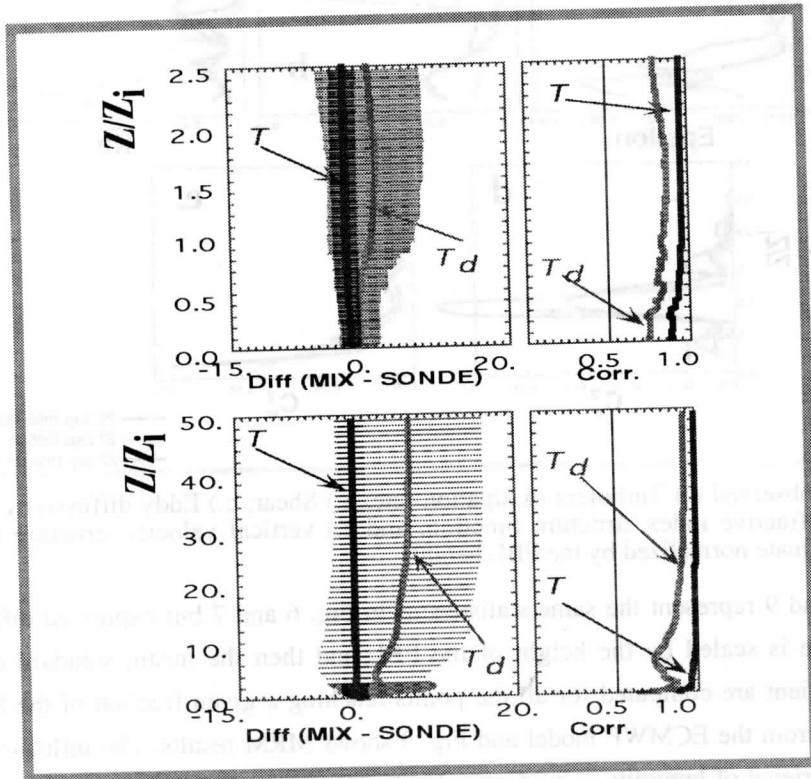


Figure 9. MRM profile comparison with radiosonde profiles for all 20 cases. The mean (thick solid line) and standard deviations (thin, horizontal solid lines) of the differences and the correlation coefficient (thick solid line) for all levels  $Z$  normalized to the PBL height  $Z_i$ . Top  $Z/Z_i = 2.5$ . Bottom  $Z/Z_i = 50$ .

#### 4.2 Humidity Gradient Statistics

Figure 5 shows the statistics obtained for all 20 cases of radar-observed and radiosonde-computed humidity gradient profiles. The vertical coordinate is scaled by the PBL height to provide better comparison since the PBL depth varied significantly over the experimental period. It is evident that the wind profiling radars do measure humidity gradient profiles.

#### 4.3 Humidity and Temperature

Figures 6 and 7 show the statistics for the humidity and temperature for all the 20 cases. Fig. 6 refers to ECMWF model analysis profiles for the nearest grid point and Fig. 7 refers to the MRM profiles. Mean, standard deviation, and correlation coefficient are listed above the scatter plots for each variable. The ECMWF temperature scatter plot shows a larger spread at about 20 (°C) which indicates lack of vertical resolution at the PBL top. MRM humidity (dewpoint) profiles show very little spread at the same temperature indicating improvements obtained from the humidity gradient measurements. However, at the temperature in -35 (°C) to -95 (°C) range MRM dewpoints are showing warm bias compared to the radiosonde dewpoints. This is a result of having no additional moisture information at mid-altitudes. Such information can be obtained either with the more powerful radar or by using commercial airline program equivalent to the ACARS program but to observe humidity in mid-altitudes .

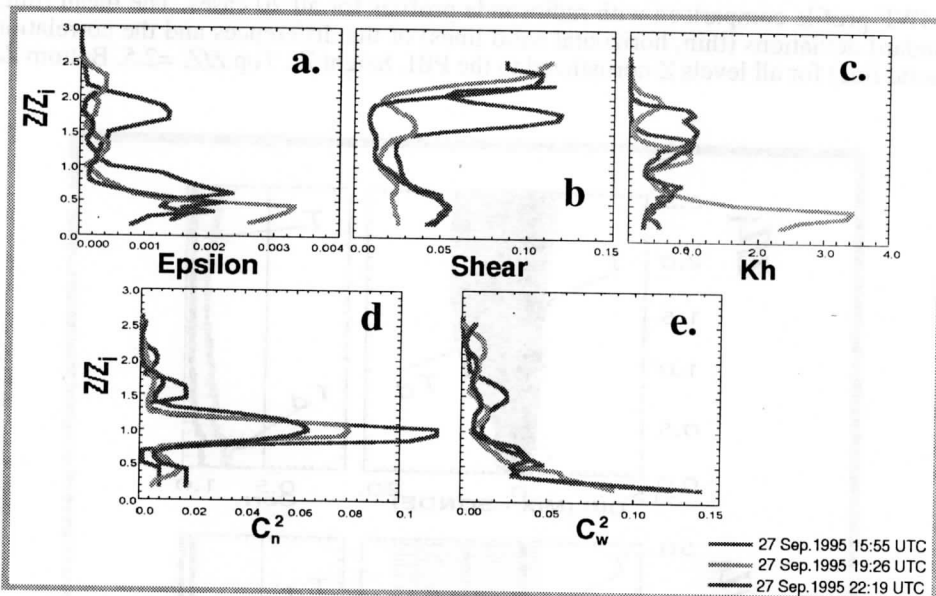


Figure 10. Radar-observed a.) Turbulent dissipation rate, b.) Shear, c.) Eddy diffusivity for moisture/heat, d.) refractive index structure function, and e.) vertical velocity structure function. Vertical coordinate normalized by the PBL height.

Figures 8 and 9 represent the same statistics as in Fig. 6 and 7 but expressed differently. Here the vertical coordinate is scaled by the height of the PBL and then the mean, standard deviation and the correlation coefficient are computed for all the points reaching a given fraction of the PBL depth. Fig. 8 shows the results from the ECMWF model and Fig. 9 shows MRM results. The influence of the humidity gradient on the retrieval of humidity is evident in Fig.9. The mean, standard deviation, and the correlation coefficient for the dewpoint within the PBL are greatly improved.



#### 4.4 PBL Application

Obtaining accurate measurements of the moisture and heat fluxes across the PBL is important for the NWP models because these fluxes drive the general circulation of the atmosphere. Most models use various turbulence parameterization schemes to express the effect of unresolved, subgrid scale motions in terms of the mean quantities such as temperature or humidity. However, because radars can measure the turbulent dissipation rate,  $\varepsilon$ , within the pulse volume, it is possible to compute the turbulent eddy diffusivity,  $K_{\phi,H}$  (for moisture or heat, Eq. 3) from the raw radar measurements.  $B_{\phi,H}$  and  $B_w$  in Eq. 3 are empirical Kolmogorof constants (for moisture or heat, and vertical velocity).

$$K_{\phi,H} = \frac{\varepsilon}{\left(\frac{d\bar{u}}{dz}\right)^2 \frac{B_{\phi,H}}{0.7B_w}} \quad (3)$$

Radar-observed eddy diffusivity can be used from the first gate and up. The parameterization schemes can then still be used from the ground surface to the first gate. Figure 10 shows an example of the eddy diffusivity computed from the radar measurements for three cases during the Point Loma experiment when the PBL depth was over 700 m so that it contained a larger number of radar observations within the PBL.

#### 5. CONCLUSIONS

- ◆ MRM provides humidity and temperature profiles from combining diverse ground- and space-based remote sensing measurements with improved accuracy.
- ◆ GPS water vapor measurements successfully replace microwave radiometer measurements of integrated water vapor within MRM.
- ◆ Radar measurements of  $dQ/dz$  profiles significantly improve the MRM humidity profiles. (Work is in progress to eliminate data noise problems by quality controlling the raw spectra instead of raw moment measurements.)
- ◆ Including radar  $dQ/dz$  and RASS temperature measurements into the one-dimensional variational analysis schemes used in numerical weather prediction models can improve model's humidity and temperature profiles.
- ◆ As the number of wind profiler/RASS sites grows around the globe, independent radar measurements of eddy diffusivities ( $K_M$ ,  $K_H$ ) can be used instead of various PBL parameterization schemes within the numerical weather prediction models.

#### REFERENCES

- Dabberdt, W.F., and T. W. Schlatter, 1996: Research opportunities from emerging atmospheric observing and modeling capabilities. *Bull. Am. Meteor. Soc.*, **77**, 305-323.

- Eyre, J.R., G.A. Kelly, A.P. McNally, E. Andersson, and A. Persson, 1993: Assimilation of TOVS radiance information through one-dimensional variational analysis. *Quart. J. Roy. Meteor. Soc.*, **11**, 1427-1463.
- Gossard, E. E., D. E. Wolfe, K.P.Moran, R.A. Paulus, K.D. Anderson, and L.T. Rogers, 1997: Measurement of clear-air gradients and turbulence properties with ground-based Doppler radars, Submitted to *J. Atmos. Ocean. Technol.*,
- McNally, A.P., G.A. Kelly, J.R. Eyre, and E. Andersson, 1994: Experiments using one-dimensional variational analysis of TOVS data at ECMWF., *Proc. ECMWF/EUMETSAT Seminar on "Developments in the use of satellite data in numerical weather prediction"*; Reading, UK; 6-10 Sept. 1993; ECMWF Report, 221-232.
- Smith, W. L., 1985: Satellites. Handbook of Applied Meteorology, Ed. David d. Houghton. *John Wiley & Sons.*, New York., 380-472.
- Stankov, B. B., 1996: Ground- and space-based temperature and humidity retrievals: Statistical evaluation. *J. Appl. Meteor.*, **35**, 444-463.
- Stankov, B. B., E. R. Westwater, and E. E. Gossard, 1996: Use of wind profiler estimates of significant moisture gradients to improve humidity profile retrieval. *J. Atmos. Ocean. Technol.*, **13**, 1285-1290.
- Starr, D. O'C. and S. H. Melfi, 1991: The Role of Water Vapor in Climate: A Strategic Plan for the Proposed GEWEX Water Vapor Project (GVaP). *NASA Conf. Publ.* 3120, National Aeronautics and Space Administration, Washington, D.C., 50 pp.
- Velleman, P.F. and D.C. Hoaglin, 1981: *Applications, Basics, and Computing of Exploratory Data Analysis*. Duxbury Press, Boston, Massachusetts.
- Westwater, E. R., 1993: Ground-based remote sensing of meteorological variables. *Atmospheric Remote Sensing by Microwave Radiometry*. M. A. Janssen Ed., J. Wiley & Sons. 145-213.
- Wolfe, D. E., et al., 1997: An operational water vapor remote sensing network using global positioning system receivers: Network design and preliminary results. *J. Atmos. Ocean. Tech.* (In review)

**TECHNICAL PROCEEDINGS OF  
THE NINTH INTERNATIONAL TOVS STUDY CONFERENCE**

Igls, Austria

20-26 February 1997

Edited by

J R Eyre

Meteorological Office, Bracknell, U.K.

Published by

European Centre for Medium-range Weather Forecasts  
Shinfield Park, Reading, RG2 9AX, U.K.

May 1997